

We thank Referee #2 for the careful manuscript reading. Below we will address the individual comments.

COMMENT

General comments

Wagner et al. describe experiments in the AIDA cloud chamber on a microphysical process termed "pore condensation and freezing mechanism" (PCF). This process leads to preactivation of certain types of aerosol once they have temporarily experienced temperatures some degrees lower than 237 K, the spontaneous freezing limit of pure water. The process works even although neither water nor ice saturation was achieved during the cooling process. The reason for this is the negative Kelvin effect in appropriate pores or between structural elements of the aerosol particles which substantially lowers the saturation water vapour pressure so that condensation can proceed at ambient vapour pressures much lower than saturation (with respect to a plane water surface).

The paper is quite interesting but hard to read. The reason for this trouble is the great amount of detail that must be provided for every experiment. Fortunately, there are several appendices where additional details are transferred to. Because of this it is particularly necessary that the theoretical principles are explained clearly. In the following I would like to make some suggestions for modifications that would to my view make the theoretical part more concise, hence clearer.

The paper is an appropriate contribution to ACP.

Specific comments and suggestions

Description of the theory

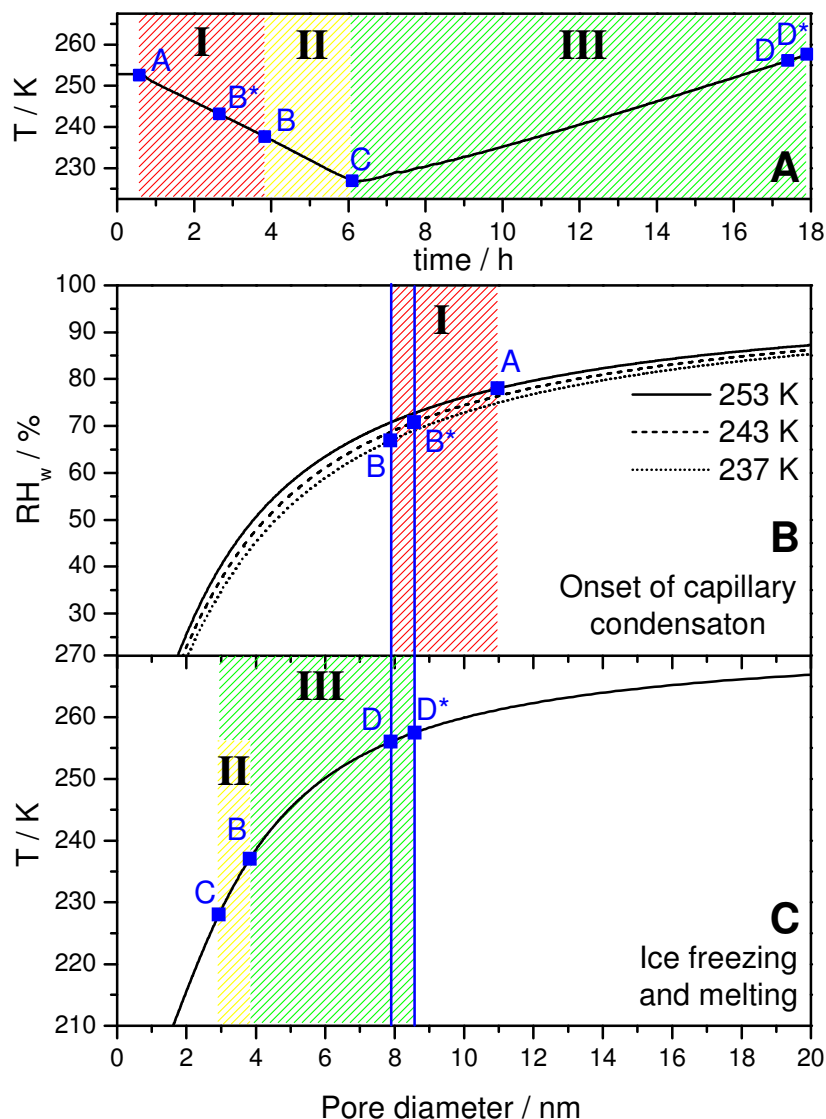
In principle, the PCF process is easy to understand. First we need condensation of liquid water in a pore under water-subsaturated conditions. This is possible because of the negative Kelvin-effect (i.e. Kelvin effect with negative radius of curvature), which effectively lowers the saturation vapour pressure. The radius of curvature is determined by the temperature and the actual relative humidity. It is proportional to the pore dimension, and thus it sets a maximum pore dimension for which condensation is just possible. Then we need freezing of the liquid, which is only possible if the pore size is larger than the critical ice germ size, again dependent on temperature, which sets the lower pore radius. Thus the range of pore sizes is set by the two described conditions. Although all this is mentioned in the paper, it is to my taste too dispersed and thus the reason why only a certain pore size range can cause the observed effects can easily be overlooked. For instance, the abstract only mentions the appropriate range, 3-8 nm, without any explanation. For readers that only read the abstract it is not possible to understand why exactly this is the appropriate range. Nobody will remember the values later, but a concise explanation can be memorised. I suggest that such a short summary of how the processes set the size boundaries of the pores is provided, perhaps in 4.1 before the details with formulas etc. are explained in the following subsections. In the abstract, one sentence like "this range is set by a combination of requirements from the negative Kelvin effect for condensation and a critical size of ice germs for ice growth" will suffice.

ANSWER

It is a good suggestion to extend the introductory remarks in Sect. 4.1 in order to better highlight the three different processes that occur during our temperature-cycling experiments, namely (I) pore condensation of supercooled water, (II) freezing of pore-contained water, and (III) melting of ice in the pores, and how these processes control the range of pore diameters involved in the PCF pre-activation experiments. We have revised the manuscript text accordingly, as shown below. Following the referee's suggestion, we have added in the abstract on page 29000, line 18 the statement:

“This range is set by a combination of requirements from the negative Kelvin effect for condensation and a critical size of ice embryos for ice nucleation and melting.”

As discussed in our answer to Referee #1, we have also modified Fig. 5 to illustrate the different stages of the pre-activation experiments and their analysis more clearly. The revised version is shown here:



In panel A, we use a colour coding to illustrate the three different processes/stages of the experiment. The red-hatched area (period I) addresses the capillary condensation of supercooled

water when the AIDA chamber is cooled from 253 to 237 K with constant $RH_{ice} = 95\%$. This process is analysed in panel B based on the negative Kelvin effect. Process II is the freezing of the liquid in the pores when cooling the AIDA from point B to point C, which is analysed by the temperature-dependent pore ice stability curve shown in panel C. The same curve applies for describing the melting of ice in the pores when again increasing the AIDA temperature from point C to points D/D* (period III).

The following four comments from Referee #2 also deal with Sect. 4.1; so we will first address these issues and then present our revised Sect. 4.1.

COMMENT

Other comments and questions on Section 4

1) Marcolli (2014) introduced the term "inverse" Kelvin effect, and it is used here as well. But the notion "inverse" is not explained, neither by Marcolli nor here. Probably it refers to the negative curvature of the water meniscus in a pore, and then it might be better to use "negative" Kelvin effect. As it also induces condensation at negative (!) supersaturation, not inverse supersaturation, I suggest to replace "inverse" by "negative".

ANSWER

Indeed, if the curvature of the water meniscus is negative, condensation can already occur at subsaturation levels. The term "inverse Kelvin effect" appears in previous papers co-authored by Marcolli, e.g. in Sjogren et al. (2007), and its use is motivated because the concavity of the water surface in a pore results in a Kelvin effect that is inverse compared to a convex liquid droplet. Mathematically, this is taken into account by adding a minus sign to the argument of the exponential of the Kelvin equation – so we agree that it is better to speak of a "negative" Kelvin equation.

We have used the term "negative Kelvin equation" in the introductory part of Sect. 4.1 and have modified the first sentences of Sect. 4.1.1 as follows:

"The concavity of the water surface in a pore results in a Kelvin effect that is inverse compared to a convex liquid droplet, meaning that water condensation can already occur at $RH_w < 100\%$ (Sjogren et al., 2007). Quantitatively, this is taken into account by adding a minus sign to the argument of the exponential of the Kelvin equation (Eq. 1)."

Sjogren, S., Gysel, M., Weingartner, E., Baltensperger, U., Cubison, M. J., Coe, H., Zardini, A. A., Marcolli, C., Krieger, U. K., and Peter, T., Hygroscopic growth and water uptake kinetics of two-phase aerosol particles consisting of ammonium sulfate, adipic and humic acid mixtures, *J. Aerosol Sci.*, 38, 157-171, 2007.

COMMENT

2) Why is it the surface tension between water and air that appears in Eq. 1 and not the surface tension between water and the pore wall? And how is the radius of curvature of the water meniscus related to the pore size. I have the impression that these two (generally different) quantities are taken to be equal in section 4.1.1.

ANSWER

For calculating the water vapour pressure over the curved water meniscus, it is indeed the surface tension of the air-water interface that has to be considered in the Kelvin equation, see e.g. the Pruppacher and Klett (1997) reference. The pore wall, or more specifically the wettability of the pore wall, is important for the second issue raised by the referee. The traces depicted in Fig. 5B were indeed computed assuming that the radius of curvature of the water meniscus is equal to the pore radius. This is of course only true for fully wettable capillaries with a zero contact angle. We have made this clear in the revised manuscript text by explicitly introducing the contact angle in the description of the Kelvin equation. The text after Eq. (1) now reads:

$$\frac{e_w}{e_{sat,w}} = \exp\left(-\frac{2M_w\sigma_{w/a}}{RT\rho_w a}\right) \quad (1)$$

“Eq. (1) describes the reduction of the saturation water vapour pressure over a concave water meniscus, e_w , in relation to that over a flat water surface, $e_{sat,w}$ (Pruppacher and Klett, 1997). The quotient $e_w/e_{sat,w}$ equals the saturation ratio of moist air with respect to a plane water surface. M_w is the molecular weight of water, $\sigma_{w/a}$ the surface tension for a water-humid air interface, R the universal gas constant, ρ_w the density of water, T the absolute temperature, and a the radius of curvature of the water surface in a capillary. For a circular capillary, a is equal to $D/(2\cos\Theta)$, where D is the pore diameter and Θ the contact angle between water and the pore wall (Fukuta, 1966). In the case of fully wettable capillaries with a zero contact angle, the radius of curvature is equal to the pore radius.”

We further added a statement that the calculations shown in Fig. 5B were done assuming a zero contact angle. At the end of Sect. 4.1.3, we then explore the changes in our calculations if we would employ a non-zero contact angle. Note that we have no information at all about the contact angles between water and the pore walls of our investigated particles. We found some measurements for several clay minerals in the literature (Janczuk and Bialopiotrowicz, 1988), indicating that Θ is rather low with $\leq 30^\circ$. With $\Theta = 30^\circ$, we have redone our computations to test the impact on the range of pore diameters involved in the PCF pre-activation experiments. This new analysis, added at the end of Sect. 4.1.3, reads as follows:

“Whereas heterogeneous freezing would increase the temperature threshold for the loss of the pre-activation ability, the opposite behaviour would be encountered if the capillaries of the porous materials were only partially wettable. Here, the factor $\cos\Theta$ would be less than unity, meaning that the radius of curvature of the water meniscus would be larger than the pore radius, thereby reducing the Kelvin effect. The maximum pore size for water condensation would diminish, and hence the upper threshold temperature for the disappearance of the pre-activation behaviour would decrease.

Accurate values for the contact angles between water and the pore walls of our investigated particles are not available. Rather low Θ values of equal or less than 30° were found for several clay minerals (Janczuk and Bialopiotrowicz, 1988). In order to estimate the effect of a non-zero contact angle, we have redone our calculations for a contact angle of 30° . This reduces the 8 nm size threshold for capillary condensation at 237 K to about 6.8 nm, yielding 253 K instead of 257 K as the upper temperature for the loss of pre-activation.”

Janczuk, B., and Bialopiotrowicz, T., Components of Surface Free-Energy of Some Clay-Minerals, Clay Clay Miner., 36, 243-248, 1988.

So it can be seen that the impact on the upper threshold temperature is not too large if one considers rather small, non-zero contact angles. The situation might be different for soot particles where the contact angles might be higher than for mineral particles (Persiantseva et al., 2004). This could further reduce the upper threshold temperature for the loss of pre-activation, as was actually observed in our pre-activation data for GSG soot particles where the improved ice nucleation ability already disappeared above 250 K. We have added a respective statement to our discussion on page 29017, line 5:

“The pre-activation mode of the fractal GSG soot particles already disappeared above 250 K, i.e., at a temperature somewhat lower than observed for the CBV400, diatomaceous earth, and illite NX particles. This might be due to the fact that water contact angles on soot surfaces tend to be higher than for mineral surfaces (Persiantseva et al., 2004), thereby lowering the temperature threshold for the loss of the pre-activation behaviour (see Sect. 4.1.3).”

Persiantseva, N. M., Popovicheva, O. B., and Shonija, N. K., Wetting and hydration of insoluble soot particles in the upper troposphere, *J. Environ. Monit.*, 6, 939-945, 2004.

COMMENT

3) Point B* in the diagrams: How can water in the pores freeze heterogeneously when there is a quasi-liquid layer between the ice and the pore wall? Doesn't this exclude the possibility of heterogeneous nucleation?

ANSWER

Good question – Marcolli (2014) mentions several studies where freezing and melting of ice were insensitive to variations of the surface properties of the pore walls. However, this issue is controversially discussed: Referee #1 of Marcolli's paper e.g. argued that *“one would expect a layer of bound water 0.6 nm thick at temperatures well below 0 degC to be very different from bulk water and to reflect the pore wall characteristics.”* So one might also argue that the bounded or adsorbed water layer actually mediates the properties of the crystalline substrate into the bulk of water, and is thus absolutely essential for the heterogeneous nucleation of ice (because there is no direct match between the crystalline lattice of most minerals and ice). We have added the following statement to Sect. 4.1.3 to make clear that the occurrence of heterogeneous freezing remains uncertain:

“The suggestion of heterogeneous freezing is, however, somewhat speculative because repeatedly a non-freezing layer of bound water next to the pore walls was found. Therefore, it remains unclear whether the material of the pore wall can actually trigger the freezing of the free water in the pore space. Marcolli (2014) summarised several studies where freezing and melting of ice were insensitive to variations of the surface properties of the pore walls. However, heterogeneous freezing could explain some of our observations, as discussed in Sect. 4.2.”

Similarly, we have modified the following statement from Sect. 4.2 (page 29016, line 15, changes in red):

“This heterogeneous ice nucleation mode, **if mediated by the non-freezing layer of bound water next to the pore walls**, could increase the freezing temperature of the capillary-held water during pre-activation (freezing at point B* instead of B), and thereby increase the upper melting temperature of ice in the pores (melting at point D* instead of D).”

COMMENT

4) I was wondering why condensation in the pores that commences already at your starting T (253 K) in pores with $D < 11$ nm, does not lead to a size range 3-11 nm. Instead, the maximum pore dimension is 8 nm, which refers to 237 K. How can one explain this. Does the water in the larger pores (8-11 nm) evaporate before it can freeze?

ANSWER

Yes, we assume that water in larger pores (8 – 11 nm) evaporates before it can freeze below 237 K. We have clarified this issue in the revised manuscript text as follows:

“Point A in Fig. 5B represents the starting point of the experimental trajectory, denoting the prevalent value of RH_w when the aerosol particles were injected into the chamber at a temperature of 253 K (corresponding to $RH_{ice} = 95\%$ at the same temperature). Here, the maximum diameter of fully wettable pores that can fill with water is about 11 nm. When the AIDA chamber is cooled at constant RH_{ice} of 95% to the homogeneous freezing temperature of supercooled water at 237 K (point B), the relative humidity with respect to supercooled water decreases, meaning that water in larger pores evaporates before it can freeze. When approaching 237 K, capillary-held supercooled water will only be retained in pores with diameters smaller than about 8 nm.”

In the following, we show our new Sect. 4.1 with all revisions included (changes compared to the original version highlighted in red):

4.1 Overview: Theoretical considerations on the water condensation, freezing, and melting of ice in pores

Fig. 5A shows the time series of the AIDA temperature during a typical pre-activation experiment. We have used a colour coding to discriminate between the three individual processes that have to be considered for the interpretation of the observed pre-activation behaviour. Process I (red-hatched area) is the capillary condensation of supercooled water when the AIDA chamber is cooled from 253 K (starting temperature for aerosol injection, point A) to 237 K (homogeneous freezing temperature of supercooled water, point B). Process II (yellow-hatched area) is the freezing of capillary-held water when the AIDA temperature is further reduced from 237 to 228 K (point C). Finally, process III (green-hatched area) is the melting of ice in the capillaries when again increasing the temperature of the AIDA chamber. The humidity and temperature conditions for the occurrence of these three processes depend on the pore diameter. Process I is quantitatively analysed based on the negative Kelvin equation that determines the onset of capillary condensation as a function of the pore size

(Fig. 5B). This sets a maximum pore dimension for which condensation is just possible at the prevailing RH_w in the AIDA chamber. Process II is analysed based on the temperature-dependent pore ice stability curve (Fig. 5C), which is derived from the critical embryo size for homogeneous ice nucleation as defined in Classical Nucleation Theory. This sets a minimum pore dimension for which freezing of the liquid is possible at the given AIDA temperature. The same curve (Fig. 5C) applies for process (III), the melting of ice in the pores. This analysis yields the maximum temperature for which the pre-activation ability by the PCF mechanism can still be observed in the AIDA chamber. In the following three sections, we outline the details of our calculations.

4.1.1 Process I: Capillary condensation of supercooled water

The concavity of the water surface in a pore results in a Kelvin effect that is inverse compared to a convex liquid droplet, meaning that water condensation can already occur at $RH_w < 100\%$ (Sjogren et al., 2007). Quantitatively, this is taken into account by adding a minus sign to the argument of the exponential of the Kelvin equation (Eq. 1).

$$\frac{e_w}{e_{sat,w}} = \exp\left(-\frac{2M_w\sigma_{w/a}}{RT\rho_w a}\right) \quad (1)$$

Eq. (1) describes the reduction of the saturation water vapour pressure over a concave water meniscus, e_w , in relation to that over a flat water surface, $e_{sat,w}$ (Pruppacher and Klett, 1997). The quotient $e_w/e_{sat,w}$ equals the saturation ratio of moist air with respect to a plane water surface. M_w is the molecular weight of water, $\sigma_{w/a}$ the surface tension for a water-humid air interface, R the universal gas constant, ρ_w the density of water, T the absolute temperature, and a the radius of curvature of the water surface in a capillary. For a circular capillary, a is equal to $D/(2\cos\Theta)$, where D is the pore diameter and Θ the contact angle between water and the pore wall (Fukuta, 1966). In the case of fully wettable capillaries with a zero contact angle, the radius of curvature is equal to the pore radius.

As shown by Marcolli (2014), the measured onset relative humidities for the capillary condensation of water in pores of different mesoporous materials can adequately be described by Eq. (1). We have therefore used this equation to calculate the RH_w values for the onset of capillary condensation of supercooled water for three relevant temperatures to predict the upper size limit of pores that can fill with water at the RH_w conditions prevalent in the AIDA chamber (Fig. 5B). We took into account temperature-dependent parameterisations for $\sigma_{w/a}$ and ρ_w given by Pruppacher and Klett (1997), but ignored the Tolman correction for the size dependence of surface tension (Rao and McMurry, 1990) and assumed a zero contact angle.

Point A in Fig. 5B represents the starting point of the experimental trajectory, denoting the prevalent value of RH_w when the aerosol particles were injected into the chamber at a temperature of 253 K (corresponding to $RH_{ice} = 95\%$ at the same temperature). Here, the maximum diameter of fully wettable pores that can fill with water is about 11 nm. When the AIDA chamber is cooled at constant RH_{ice} of 95% to the homogeneous freezing temperature of supercooled water at 237 K (point B), the relative humidity with respect to supercooled water decreases, meaning that water in larger pores evaporates before it can freeze. When approaching 237 K, capillary-held supercooled water will only be retained in pores with diameters smaller than about 8 nm. Homogeneous freezing could then lead to the formation of ice in such sized pores. Ice formation could also involve slightly larger pores, but this would require that the capillary-held water already freezes heterogeneously at a temperature higher than 237 K (e.g. at point B* with $T = 243$ K). We will further discuss this issue in Sect. 4.1.3.

4.1.2 Process II: Freezing of capillary-held water

In the next step, we analyse the freezing of the capillary-held water when the AIDA temperature is lowered from the homogeneous freezing limit (point B, 237 K) to the minimum temperature of 228 K (point C). In particular, it has to be examined whether the homogeneous (or heterogeneous) freezing of supercooled water is not impeded for narrow pore diameters. Marcolli (2014) has adopted a quantity from Classical Nucleation Theory to describe the

freezing and melting of ice in pores, namely the critical embryo size for homogeneous ice nucleation in the pores. Only if the pore dimension exceeds the critical embryo size, the ice embryo has a higher tendency to grow, which reduces the free energy of the system, than to shrink, which increases the free energy (Pruppacher and Klett, 1997). Ice formation should therefore be inhibited in pores where an ice embryo cannot grow beyond the critical embryo size, even if the temperature is below 237 K.

The critical radius of a spherical ice embryo for homogeneous ice nucleation, r_c , for which the Gibbs free energy of embryo formation within the liquid phase has its maximum, is given by (Murray et al., 2012):

$$r_c = \frac{2M_w \sigma_{i/w}}{RT \rho_i \ln \frac{e_{sat,w}}{e_{sat,i}}} \quad (2)$$

In Eq. (2), $\sigma_{i/w}$ is the interfacial tension between water and the ice embryo, ρ_i the density of ice, and $e_{sat,i}$ the saturation water vapour pressure over a flat ice surface. Using Eq. (2), we have calculated the temperature-dependent pore diameters needed to incorporate a critical ice embryo as $2r_c + 2t$, where t accounts for a non-freezing quasi-liquid layer between pore wall and ice embryo (Marcolli, 2014). In this computation, t was set to 0.6 nm (Marcolli, 2014), temperature-dependent ρ_i values were obtained from the parameterisation given by Pruppacher and Klett (1997), $e_{sat,w}$ and $e_{sat,i}$ were calculated according to the formulations by Murphy and Koop (2005), and $\sigma_{i/w}$ was taken from the fit of measured homogeneous ice nucleation rate coefficients presented by Zobrist et al. (2007).

The result of the computation is shown in Fig. 5C. Regarding our pre-activation experiments, this curve defines the lower threshold size of pores where ice formation due to freezing of capillary-held water can occur at a given temperature. **The yellow-hatched area defines the temperature range of process II as defined in Fig. 5A.** At 237 K (point B), the minimum pore size threshold for freezing of the liquid is about 4 nm, and it further decreases

to about 3 nm at 228 K, the minimum temperature during the experiment (point C). Here, all aerosol particles with pores in the diameter range from 3 to 8 nm therefore have the chance to incorporate ice due to the PCF mechanism even in an ice-subsaturated environment. **3 nm is the minimum pore size in which capillary-held water can freeze, and 8 nm is the maximum pore size in which condensation of supercooled water has been possible.** These ice pockets can trigger the depositional ice growth mode when the aerosol particles are directly probed in an expansion cooling experiment started at 228 K. In our pre-activation experiments, however, we want to investigate the survival of such ice pockets and their contribution to depositional ice growth at warmer temperatures. Therefore, we have to consider as the third important process the melting of ice when increasing the temperature in the pre-activation experiments (**process III, green-hatched areas in Figs. 5A and C**).

4.1.3 Process III: Melting of ice in pores

For describing the temperature dependence of the melting of ice in pores, the same curve as for the freezing of ice applies (Marcolli, 2014). Once the diameter of a certain pore gets smaller than the critical embryo size during warming, the ice in the pore should melt because shrinkage of the ice phase would lead to a decrease in the free energy of the system. Point D at 257 K (Fig. 5C) therefore denotes the melting temperature of ice in the largest pores in which ice pockets could have been formed via the PCF mechanism in the case of homogeneous freezing at point B. Above that temperature, the pre-activation behaviour should disappear. In the case of heterogeneous freezing at point B*, the temperature threshold for the disappearance of the pre-activation ability could be a few degrees higher (point D*), because ice in larger pores with a higher melting temperature were present. **The suggestion of heterogeneous freezing is, however, somewhat speculative because repeatedly a non-freezing layer of bound water next to the pore walls was found. Therefore, it remains unclear whether the material of the pore wall can actually trigger the freezing of the free water in the pore space. Marcolli (2014) summarised several studies where freezing and melting of ice were**

insensitive to variations of the surface properties of the pore walls. However, heterogeneous freezing could explain some of our observations, as discussed in Sect. 4.2.

Whereas heterogeneous freezing would increase the temperature threshold for the loss of the pre-activation ability, the opposite behaviour would be encountered if the capillaries of the porous materials were only partially wettable. Here, the factor $\cos\Theta$ would be less than unity, meaning that the radius of curvature of the water meniscus would be larger than the pore radius, thereby reducing the Kelvin effect. The maximum pore size for water condensation would diminish, and hence the upper threshold temperature for the disappearance of the pre-activation behaviour would decrease.

Accurate values for the contact angles between water and the pore walls of our investigated particles are not available. Rather low Θ values of equal or less than 30° were found for several clay minerals (Janczuk and Bialopiotrowicz, 1988). In order to estimate the effect of a non-zero contact angle, we have redone our calculations for a contact angle of 30° . This reduces the 8 nm size threshold for capillary condensation at 237 K to about 6.8 nm, yielding 253 K instead of 257 K as the upper temperature for the loss of pre-activation.

COMMENT

Minor comments

1) P. 29001, ll. 4-5: "an even smaller fraction" should be quantified.

ANSWER

We propose to point to the INP measurements for various geographic locations summarised in Pruppacher and Klett (1997) (Fig. 9-17 therein). There is typically a decrease in the INP number concentration by about two orders of magnitude when the temperature is increased from -20 to -10°C . We have added a respective statement to our manuscript text:

"Amongst this subset, an even smaller fraction of aerosol particles can trigger the glaciation of supercooled cloud droplets at temperatures higher than 258 K. INP measurements for various geographic locations indicate that the INP number concentration typically decreases by two orders of magnitude when the temperature increases from 253 to 263 K (Pruppacher and Klett, 1997). Most of the INPs that are active above 258 K are supposed to be composed of biological material (Murray et al., 2012; Prenni et al., 2009)."

COMMENT

2) P. 29001, ll. 14-15: correct hyphenation of "represent".

ANSWER

We will pay attention when proof-reading the revised manuscript that the hyphenation is correct.

COMMENT

3) P. 29002, ll. 10-11: "INPs that have crystallized...". It is unclear whether these are ice crystals or other crystals that contain crystal water.

ANSWER

We have specified this issue by stating: "...which involves temperature cycling of INPs composed of solid organic and inorganic crystals that have crystallised from aqueous solution droplets." So it becomes clear that other crystals that contain crystal water are meant.

COMMENT

4) Section 3.1: It is reported that the unprocessed CBV400 starts nucleating ice at $RH_i=102\%$ and that this is probably not due to deposition nucleation but due to pre-activation following the PCF process pathway. I do not understand this argument: when the aerosol is unprocessed, as stated, how can it simultaneously be pre-activated?

ANSWER

We do not state that the unprocessed CBV400 particles that are directly injected at 228 K and nucleate ice at $RH_i=102\%$ are subject to "pre-activation following the PCF pathway". The term pre-activation is exclusively reserved for particles that are subjected to temperature cycling and then show an improved ice nucleation ability at warm temperatures. We only state here that the unprocessed CBV400 particles are subject to the PCF mechanism, i.e., ice pockets can instantly form when the particles enter the AIDA chamber at 228 K and $95\% RH_{ice}$, thereby explaining their very high ice nucleation ability. To make this clearer, we have slightly re-phrased our statement on page 29009, line 2 as follows:

"More likely, the ice nucleation mode evident in Fig. 3B is due to the depositional growth of ice pockets which already form by the PCF mechanism after injecting the CBV particles into the AIDA chamber at 228 K and $RH_{ice} = 95\%$."

COMMENT

Figures: As water saturation is important for your explanations, RH with respect to liquid water should be indicated as well in your figures (in addition to RH wrt ice).

ANSWER

Yes, we will also indicate the RH_w time series in the revised manuscript version.

COMMENT

Figure 5c: red hatching not visible in my printed version.

ANSWER

We have completely revised Fig. 5 and increased the thickness of the hatched lines to make them better visible.

Best wishes,

Robert Wagner and co-authors